Soft Matter

Cite this: *Soft Matter*, 2011, **7**, 2332

www.rsc.org/softmatter

COMMUNICATION

Optimized monotonic convex pair potentials stabilize low-coordinated crystals

É. Marcotte,[a] F. H. Stillinger[b] and S. Torquato*[abc]

Received 26th October 2010, Accepted 13th January 2011
DOI: 10.1039/c0sm01205j

We have previously used inverse statistical-mechanical methods to optimize isotropic pair interactions with multiple extrema to yield low-coordinated crystal classical ground states (*e.g.*, honeycomb and diamond structures) in *d*-dimensional Euclidean space $\mathbb{R}^d$. Here we demonstrate the counterintuitive result that no extrema are required to produce such low-coordinated classical ground states. Specifically, we show that monotonic convex pair potentials can be optimized to yield classical ground states that are the square and honeycomb crystals in $\mathbb{R}^2$ over a non-zero number density range. Such interactions may be feasible to achieve experimentally using colloids and polymers.

The forward approach of statistical mechanics focuses on finding the structure and macroscopic properties of many-particle systems with specified interactions. This approach has led to the discovery of rich and complex many-particle configurations.[1–3] The power of the inverse statistical-mechanical approach is that it can be employed to design interactions that yield a targeted many-particle configuration with desirable bulk physical properties.[4] This work continues our general program to use inverse approaches to optimize pair interactions to achieve novel targeted classical ground-state configurations in *d*-dimensional Euclidean space $\mathbb{R}^d$. In particular, we have found optimized pair interactions that yield low-coordinated crystal classical ground states (*e.g.*, square and honeycomb crystals[5] in $\mathbb{R}^2$, and simple cubic[6] and diamond[7] crystals in $\mathbb{R}^3$), materials with negative thermal expansion,[8] negative Poisson's ratio[9] and designed optical properties.[10] We envision using colloids and/or polymers to realize such designed potentials because one can tune their interactions.[4,11–13]

Earlier uses of the inverse approach[5] did not regard experimental feasibility as a constraint. These investigations allowed a largely unconstrained class of spherically symmetric pair potentials. In some instances in which the goal was to target low-coordinated crystal ground states, it was shown that only a few potential wells were required,[5,7] which nonetheless may be difficult to realize experimentally. If purely repulsive short-ranged monotonic pair potentials existed that could achieve unusual many-particle ground states, they would be easier to produce experimentally, albeit under positive pressure. However, encoding information in monotonic potentials to yield low-coordinated ground-state configurations in Euclidean spaces is highly nontrivial. Such potentials must not only avoid close-packed (highly coordinated) competitors but crystal configurations that are infinitesimally close in structure (very slight deformations of the targeted low-coordinated crystal), which is a great challenge to achieve *theoretically* while maintaining the monotonicity properties.

In this communication, we use a *modified* inverse approach to obtain monotonic *convex* potentials whose ground states in $\mathbb{R}^2$ are either the square lattice or honeycomb crystal.[14] Thus, our work is a theoretical proof of concept that monotonic convex potentials can stabilize low-coordinated crystals.† We begin by describing briefly the procedure that we employ to optimize the monotonic convex potentials for the targeted low-coordinated crystals aided by *generalized coordination* functions; see ref. 15. This is followed by an analysis of their stability characteristics.

We consider the total potential energy $\Phi_N(\mathbf{r}^N)$ of a configuration C of N particles with positions $\mathbf{r}_1$, $\mathbf{r}_2$, … $\mathbf{r}_N$ to be given by a sum of pairwise terms:

$$\Phi_N(\mathbf{r}^N) = \sum_{i<j} v(r_{ij}), \tag{1}$$

where $v(r)$ is the isotropic pair potential and $r_{ij} = |\mathbf{r}_i - \mathbf{r}_j|$. For a targeted configuration C^* to be a ground state associated with a potential v, the total potential energy needs to satisfy the following property:

$$\Phi_N(v,C^*) \leq \Phi_N(v,C) \ \forall\, C. \tag{2}$$

By expressing the potential v as a function of M parameters a_1, …, a_M, *i.e.*, $v \equiv v(a_1, \ldots, a_M)$, it should be possible to find the optimized potential by varying the parameters until inequality (2) is satisfied for all possible configurations C. Due to the uncountably infinite number of possible configurations, it is impossible to check them all. Instead, we restrict ourselves to a subset of them, which we call the *competitor configurations* **C**. This allows us to redefine the problem as an optimization,[5] where the objective is to maximize the energy difference between the targeted configuration C^* and its closest competitor. This is done by introducing a utility variable Δ which is to be maximized while satisfying the following constraints:

[a]*Department of Physics, Princeton University, Princeton, New Jersey, 08544, USA*
[b]*Department of Chemistry, Princeton University, Princeton, New Jersey, 08544, USA*
[c]*Princeton Center for Theoretical Science, Princeton University, Princeton, New Jersey, 08544, USA*

$$\Phi_N(\upsilon(a_1,\ldots,a_M),C^*) \leq \Phi_N(\upsilon(a_1,\ldots,a_M),C) - \Delta,\ \forall\, C \in \mathbf{C}. \quad (3)$$

For a fixed potential υ, the utility variable Δ can only be as large as the smallest energy difference, $\Phi_N(\upsilon,C) - \Phi_N(\upsilon,C^*)$, between a competitor and the targeted configuration. Since the functional form υ is allowed to vary, the optimization procedure will find the potential that maximizes the energy difference between the targeted configuration and its closest competitor.

For a given targeted configuration C^*, we begin with a competitors set $\mathbf{C}$ that only includes the triangular lattice. A trial pair potential υ_1 is optimized using that set, and its putative ground state C_1 is computed using the Metropolis Monte Carlo algorithm. Namely, we attempt to determine the ground state for the trial potential υ_1 by generating an initial configuration from a Poisson point process. This configuration is then slowly annealed using the Metropolis scheme down to zero temperature. Since this algorithm cannot guarantee that the obtained configuration is the ground state, we repeat the procedure multiple times and keep the lowest-energy configuration as the *trial* ground state C_1 of the trial potential υ_1.

If the energy of C_1 is lower than that of C^* for the trial potential, it proves that C^* is not the ground state of υ_1. To discriminate against potentials with C_1 as their ground states, we add C_1 to the list of competitors $\mathbf{C}$, before optimizing a new trial potential υ_2. This procedure is repeated until we are confident that the trial-potential ground state is indeed C^*, at which point we have found our optimized potential. This method is adapted from the one presented by Cohn and Kumar,[14] with the difference being that we only add to $\mathbf{C}$ configurations that have lower energies than C^* for a given trial potential.

We restrict ourselves to $\upsilon(r)$ that are sums of $M = 12$ negative powers of r, with a cutoff at $r = R > 0$:

$$\upsilon(r) \equiv \begin{cases} \sum_{i=1}^{M} \frac{a_i}{r^i} & r \leq R, \\ 0 & r > R. \end{cases} \quad (4)$$

Additionally, we only consider continuous potentials whose first and second derivatives are also continuous at the cutoff. These two conditions guarantee that the interaction forces are continuous and that the phonon spectra can be calculated, respectively. Furthermore, a scale is imposed by setting $\upsilon(r = 1) = 1$.

The first low-coordinated crystal configuration to be targeted with our simulated-annealing optimization method is the square lattice with a nearest-neighbor distance of unity subject to the condition that $a_i \in [-1000,1000]$. These bounds are necessary for the linear problem to have a solution. We still find solutions when the bound widths are increased. The number density for such a configuration is unity (ρ equals; 1). The optimization procedure is restricted to monotonic convex pair potentials that are zero beyond a cutoff distance $r = R = 2$. We find the following optimized pair potential:

$$\upsilon(r) = \begin{cases} \left(\frac{28.424}{r} - \frac{245.756}{r^2} + \frac{786.742}{r^3} - \frac{1000}{r^4} \right. \\ \quad - \frac{24.043}{r^5} + \frac{1000}{r^6} - \frac{47.967}{r^7} - \frac{1000}{r^8} \\ \left. \quad + \frac{64.527}{r^9} + \frac{1000}{r^{10}} - \frac{712.166}{r^{11}} + \frac{151.240}{r^{12}} \right) & r \leq 2, \\ 0 & r > 2, \end{cases} \quad (5)$$

which is plotted in Fig.1(a). To confirm that the ground state of potential (5) is indeed the square lattice, we performed multiple simulated-annealing calculations. All of them resulted in either square lattices (as shown in Fig.1(b)) or slightly deformed square lattices, which energies were always higher than that of the perfect square lattice. We use $M = 12$ terms in our potential because higher M causes numerical instabilities and lower M results in potentials that only weakly discriminate against competitors. Importantly, the potential function (5) is only one example within a large class of functions that could be optimized to stabilize the square lattice.

To see intuitively why the purely repulsive potential (5) succeeds in stabilizing the square lattice consider the interactions due to the first and/or second coordination shells, the main contributors to the total energy. For the square, triangular and honeycomb crystals (with $\rho = 1$), the first coordination shell contributions to twice the total energies per particle u [$u = \sum_{j \neq 1} \upsilon(r_{1j})$ for the studied crystals] are respectively given by $4 \times \upsilon(1) = 4$, $6 \times \upsilon(1.075) = 4.762$ and $3 \times \upsilon(0.877) = 4.963$ (these can be compared to the entire function u, which is respectively 4.456, 4.764 and 5.236). We see that the lower value of the optimized potential (5) for the triangular lattice at its nearest-neighbor distance is not enough to compensate for the higher coordination number compared to the square lattice (six instead of only four). Thus, the relatively slow decrease of the potential (5) around $r = 1$ allows it to favor configurations with low coordination, even if it means having closer nearest neighbors. The lower-coordinated honeycomb crystal is also discriminated against, due the large increase of $\upsilon(r)$ for $r < 1$.

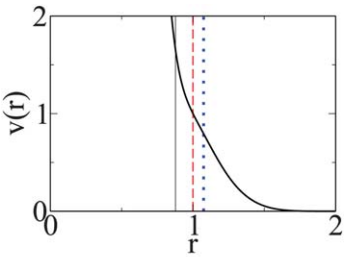

(a)

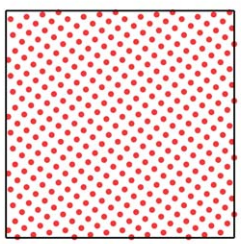

(b)

Fig. 1 (a) Optimized convex pair potential targeting the square lattice. The potential $\upsilon(r)$ at unit distance (where r is measured in terms of the nearest-neighbor distance) is taken to be unity. The vertical lines represent the nearest-neighbor distances for the honeycomb crystal (solid line), the square lattice (dashed line) and triangular lattice (dotted line) at a number density of unity ($\rho = 1$). The optimized potential ground state obtained by slowly annealing the systems starting from a fluid. The annealing was performed in a 20×20 box containing 400 particles under periodic boundary conditions. For illustration purposes, the point particles are shown to have finite sizes.

However, there are more subtle configurations that have to be discriminated against beside the aforementioned ones. These include infinitesimally close configurations, such as the rhombical and rectangular lattices. The difference in u between a rectangular lattice of aspect ratio $1+\varepsilon$ and the square lattice is equal to $\left[v'(1)/2 + \sqrt{2}v'\left(\sqrt{2}\right) + v''(1)/2\right]\varepsilon^2 + O\left(\varepsilon^3\right) = 2.551\varepsilon^2 + O\left(\varepsilon^3\right)$. The difference in u between a rhombical lattice of angle $\pi/2-\varepsilon$ and the square lattice is $\left[v'(1) + v'\left(\sqrt{2}\right)/\sqrt{2} + v''\left(\sqrt{2}\right)\right]\varepsilon^2 + O\left(\varepsilon^3\right) = 2.110\varepsilon^2 + O\left(\varepsilon^3\right)$. Stabilizing the square lattice against these two very close neighboring configurations is thus an equilibrium between having large second derivatives at the two first coordination shells, while preventing the first derivative being too negative at these two shells.

The second targeted ground-state configuration is the honeycomb crystal with a nearest-neighbor distance of unity and number density $\rho = 4/(3\sqrt{3})$. This is a more challenging ground state to achieve with a monotonic convex potential because it is only trivalently coordinated. The optimization procedure is still restricted to monotonic convex pair potentials, but the cutoff is set to $R = 3$. The optimized pair potential is given by

$$v(r) = \begin{cases} \left(\dfrac{3.767}{r} - \dfrac{48.246}{r^2} + \dfrac{230.514}{r^3} - \dfrac{451.639}{r^4} \right. \\ \quad + \dfrac{56.427}{r^5} + \dfrac{1000}{r^6} - \dfrac{868.468}{r^7} - \dfrac{776.495}{r^8} \\ \left. \quad + \dfrac{1000}{r^9} + \dfrac{521.638}{r^{10}} - \dfrac{1000}{r^{11}} + \dfrac{333.502}{r^{12}}\right) & r \le 3, \\ 0 & r > 3, \end{cases} \tag{6}$$

which is plotted in Fig.2(a). As for potential (5), we confirmed that the ground state of potential (6) is indeed the honeycomb crystal by performing multiple simulated-annealing calculations. Fig. 2(b) shows the result of one of those runs that converged to the honeycomb crystal. All final configurations other than the honeycomb crystal presented defects and had higher energies than that of the perfect honeycomb, which is strong numerical evidence that the honeycomb is indeed the ground state of potential (6).

As in the square-lattice case, the ability of the purely repulsive potential (6) to stabilize the low-coordinated honeycomb crystal lies in its slow decrease near $r = 1$. Consequently, the contributions to u from the first coordination shells of the honeycomb, triangular and square crystals [at $\rho = 4/(3\sqrt{3})$], are respectively 3, 4.077 and 3.196. The low coordination of the honeycomb crystal thus compensates for closer neighbors. The second shell energy contributions of the square and triangular lattices turn out to be larger than that for the honeycomb crystal, even if all them are relatively small due to the rapid decrease of $v(r)$. We have also verified that potential (6) discriminates against slightly sheared deformations of the honeycomb crystal, which is consistent with our phonon analysis below.

We also studied the phonon characteristics of potentials (5) and (6), *i.e.*, the mechanical response of the crystals to small deformations. Fig. 3(a) and 3(b) show the squared frequency of phonon modes as a function of their wave vectors for the square and honeycomb crystals. The absence of any negative squared frequency indicates that all of the modes have real frequency; thus, the crystals are stable under small deformations.

We have further studied the stability of our optimized potentials by exploring the effects of adding point defects to the crystals. Since defects cost energy, our targeted ground states are stable under such local modifications. We also used the newly introduced *generalized coordination functions*[15] to show that potentials (5) and (6) are part of

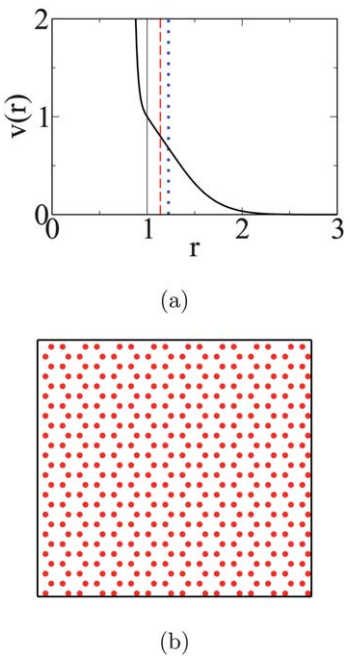

Fig. 2 As in Fig. 1, except that this is for the optimized potential targeting the honeycomb crystal. In (a) the nearest-neighbor distances are calculated for $\rho = 4/(3\sqrt{3})$; and in (b) we use 416 particles in a periodic box with dimensions $24 \times 13\sqrt{3}$.

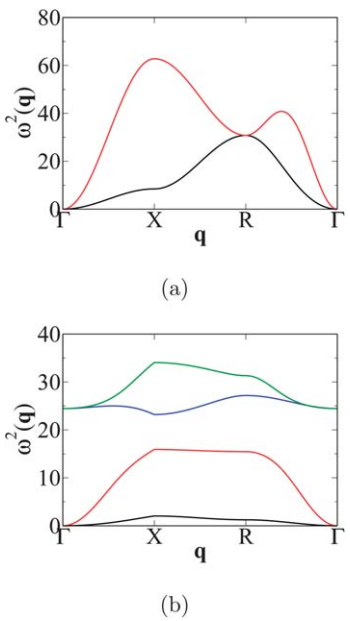

Fig. 3 Phonon spectra for the optimized potentials. The squared phonon frequency ω^2 is plotted in terms of a representative subset of phonon wave vectors **q**. Note that the spectra were calculated over the entire Brillouin zone, and no modes with imaginary frequencies were found. (a) Phonon spectrum for the "square-lattice" potential shown in Fig.1(a). (b) Phonon spectrum for the "honeycomb-crystal" potential shown in Fig. 2(a).

a large class of monotonic convex pair potentials that stabilize the square and honeycomb crystals and thus our potentials are robust against shape change. These details are given in our companion paper.[15]

Are the low-coordinated crystal ground states stable over a density range around the density values for which they are designed ($\rho = 1$ for the square lattice and $\rho = 4/(3\sqrt{3})$ for the honeycomb crystal)? We have performed both simulated-annealing ground-state calculations and computed the phonon spectra at various densities. We find that for potential (5), the square lattice is the ground state for the density range $\rho \in [0.96,1.10]$. For potential (6), the honeycomb crystal is the ground state for $\rho \in [0.74,0.80]$. Therefore, both targeted configurations can be stabilized over a non-zero number density range, which is a desirable feature for experimental realizations of our optimized potentials. This property is not at all obvious for systems under positive pressure, as there are no *a priori* reasons why deformed lattices that maintain a constant nearest neighbor distance, such as the rhomboidal and rectangular lattices, are not the ground states for densities other than the one at which the optimization was conducted.

To summarize, whether potentials exist that stabilize low-coordinated crystal ground states in Euclidean space without any potential wells is not at all obvious. We have shown that potentials without wells, namely, monotonic convex repulsive pair interactions, can counterintuitively produce low-coordinated ground states in $\mathbb{R}^2$, such as the square lattice and honeycomb crystals.

Lindenblatt *et al.*[11] have fabricated so-called "hairy colloids". These colloids are formed by grafting polymer chains onto the surface of nanoscopic microgel spheres, in a matrix of polymer chains. Manipulation of such systems offer the possibility of mimicking the interactions that stabilize the square and honeycomb crystals defined by eqns (5) and (6), respectively, although such experimental realizability remains an open fascinating question. Note that experimental feasibility should not require convexity. For example, we have also shown numerically that the square lattice can be stabilized by a monotonic non convex potential.[15] In future research, we intend to determine whether convex potentials can stabilize three-dimensional low-coordinated structures, such as simple cubic or diamond crystals.

This work was supported by the Office of Basic Energy Sciences, U.S. Department of Energy under Grant No. DE-FG02-04-ER46108. We also acknowledge support from the Natural Sciences and Engineering Research Council of Canada.

Notes and references

† We consider monotonic potentials that are also convex because this class of interactions may be amenable to rigorous analysis. Indeed, in ref. 14, Cohn and Kumar have rigorously constructed potentials that stabilize unusual targeted configurations on the surface of a d-dimensional sphere using only monotonic convex pair potentials. Restriction to compact spaces made their problem much easier to solve because their pair potentials had compact support set by the sphere radius. Nonetheless, their results are suggestive that similar proofs can be constructed in $\mathbb{R}^d$.

1 M. Watzlawek, C. N. Likos and H. Löwen, *Phys. Rev. Lett.*, 1999, **82**, 5289.
2 D. Gottwald, C. N. Likos, G. Kahl and H. Löwen, *Phys. Rev. Lett.*, 2004, **92**, 68301.
3 A.-P. Hynninen, C. G. Christova, R. Van Roij, A. Van Blaaderen and M. Dijkstra, *Phys. Rev. Lett.*, 2006, **96**, 138308.
4 S. Torquato, *Soft Matter*, 2009, **5**, 1157.
5 M. C. Rechtsman, F. H. Stillinger and S. Torquato, *Phys. Rev. E: Stat., Nonlinear, Soft Matter Phys.*, 2006, **73**, 011406.
6 M. C. Rechtsman, F. H. Stillinger and S. Torquato, *Phys. Rev. E: Stat., Nonlinear, Soft Matter Phys.*, 2006, **74**, 021404.
7 M. C. Rechtsman, F. H. Stillinger and S. Torquato, *Phys. Rev. E: Stat., Nonlinear, Soft Matter Phys.*, 2007, **75**, 031403.
8 M. C. Rechtsman, F. H. Stillinger and S. Torquato, *J. Phys. Chem. A*, 2007, **111**, 12816.
9 M. C. Rechtsman, F. H. Stillinger and S. Torquato, *Phys. Rev. Lett.*, 2008, **101**, 085501.
10 R. D. Batten, F. H. Stillinger and S. Torquato, *J. Appl. Phys.*, 2008, **104**, 033504.
11 G. Lindenblatt, W. Schärtl, T. Pakula and M. Schmidt, *Macromolecules*, 2001, **34**, 1730.
12 V. N. Manoharan, M. T. Elsesser and D. J. Pine, *Science*, 2003, **301**, 483.
13 M. P. Valignat, O. Theodoly, J. C. Crocker, W. B. Russel and P. M. Chaikin, *Proc. Natl. Acad. Sci. U. S. A.*, 2005, **102**, 4225.
14 H. Cohn and A. Kumar, *Proc. Natl. Acad. Sci. U. S. A.*, 2009, **106**, 9570.
15 É. Marcotte, F. H. Stillinger and S. Torquato, in preparation.